Engineering Notes

Initial Orbit Determination from Three Velocity Vectors

John A. Christian* and Courtney L. Hollenberg†
Rensselaer Polytechnic Institute, Troy, New York 12180

DOI: 10.2514/1.G003988

Nomenclature

$\boldsymbol{e}$	=	eccentricity vector
$\boldsymbol{h}$	=	specific angular momentum, m^2/s
$\boldsymbol{r}$	=	spacecraft position vector, m
$\boldsymbol{v}$	=	spacecraft velocity vector, m/s
$\mathcal{E}$	=	specific energy, m^2/s^2
μ	=	gravitational parameter, m^3/s^2

I. Introduction

INITIAL orbit determination (IOD) for a body following simple two-body motion is one of the classic problems in astrodynamics. Substantial prior work has been devoted to the IOD problem given three position vectors (Gibbs problem) [1,2], two position vectors and time-of-flight (Lambert's problem) [1,2], and three line-of-sight observations (e.g., methods of Laplace, Gauss, and Gooding) [3,4].

In this Note, the authors suggest a new problem to be solved: IOD using only three velocity vectors and the direction of motion (e.g., prograde or retrograde). The new problem is the complement of the Gibbs problem, in which the knowns and unknowns have been switched. In the classic Gibbs problem, three position vectors are known, and one must solve for the unknown velocity vectors at the corresponding times. Conversely, in this Note, the three velocity vectors are known, and one must solve for the unknown position vectors at the corresponding times. Like the Gibbs problem, IOD from three velocity vectors also exhibits an analytic solution.

The other obvious problem is to reimagine Lambert's problem with known velocities instead of know positions. That is, one may seek an IOD solution given only two velocity vectors, the elapsed time between these velocity observations, the direction of motion, and the number of revolutions about the central body. The authors are addressing this problem in a parallel line of work. The present Note, however, will focus exclusively on the problem of IOD from three velocity vectors.

Although any sensing technology capable of measuring inertial velocity would provide the required observations, the problem of velocity-only IOD is currently motivated by the promise of autonomous IOD using X-ray navigation (XNAV). Contemporary XNAV concepts operate by observing the X-ray signals emitted by stable millisecond pulsars [5], and a prototype system has recently been demonstrated aboard the International Space Station [6–8]. The time of arrival (TOA) of pulses may be used to determine position relative to a reference point in the direction of the source pulsar. Likewise, variation in the frequency of pulses may be used to determine inertial velocity in the direction of the source pulsar. Observations of three or more pulsars with line-of-sight directions spanning $\mathbb{R}^3$ enable three-dimensional (3D) positioning or velocity estimation. Unfortunately, the periodic nature of the pulsar signal represents a significant obstacle for using the pulse TOA-based position measurements within the IOD context, as one must solve the integer phase ambiguity problem [9]. Velocity measurements, however, do not suffer from this drawback and may be easier to obtain if no a priori information about position is available. As a consequence, velocity-only IOD is an interesting problem to consider, either by itself or as a means for removing (or constraining) the phase ambiguity problem for XNAV positioning.

The authors are hopeful that future sensing technologies (in addition to just XNAV) will be capable of producing inertial 3D velocity measurements, thus leading to a wider array of missions that could exploit the new IOD approach presented here. Perhaps the existence of an analytic velocity-only IOD method will help motivate future work in this area.

The remainder of this Note is organized as follows. Section II provides a formal statement for the problem of IOD using only three velocity vectors. Section III provides an analytic solution to this problem, while Sec. IV shows a few numerical results.

II. Problem Statement

Consider a spacecraft in orbit about a central body. Assume that the spacecraft follows two-body motion,

$$\frac{d^2}{dt^2}\boldsymbol{r} = -\frac{\mu}{\|\boldsymbol{r}\|^3}\boldsymbol{r} \tag{1}$$

where the 3×1 vector $\boldsymbol{r}$ describes the position relative to the body center and μ is the central body's gravitational constant. To simplify notation, define the velocity as $\boldsymbol{v} = \dot{\boldsymbol{r}}$.

Now, suppose that a sensor measures the velocity at three times (t_1, t_2, and t_3), producing the measurement set $\{\boldsymbol{v}_1, \boldsymbol{v}_2, \boldsymbol{v}_3\} \in \mathbb{R}^3$. A few moments of thought will reveal that one must also specify the direction of motion, as there will always be both a prograde and retrograde orbit (or, in the case of polar orbits, a clockwise and counterclockwise orbit) containing the three velocities. This fact is shown pictorially in Fig. 1.

Fully describing the orbit requires determination of the position vector associated with at least one of the velocity measurements. Therefore, one obtains the following problem statement: given a the central body's gravitational parameter μ, the direction of motion, and the velocity at three different times ($\boldsymbol{v}_1$, $\boldsymbol{v}_2$, and $\boldsymbol{v}_3$), find one (or more) of the unknown position vectors $\boldsymbol{r}_1$, $\boldsymbol{r}_2$, and/or $\boldsymbol{r}_3$.

III. Analytic IOD Solution

The key to most IOD solutions for the two-body problem is enforcement of the integrals of motion. The present work is no exception to this rule. This particular problem requires consideration of the specific angular momentum, the specific energy (*vis viva* integral), and the eccentricity vector. Therefore, recall (e.g., from [1]) that the specific angular momentum $\boldsymbol{h}$ is given by

$$\boldsymbol{h} = \boldsymbol{r} \times \boldsymbol{v} \tag{2}$$

the specific energy $\mathcal{E}$ is given by

Received 26 July 2018; revision received 12 September 2018; accepted for publication 24 September 2018; published online 26 November 2018.

*Assistant Professor, Department of Mechanical, Aerospace, and Nuclear Engineering. Senior Member AIAA.

†Graduate Research Assistant, Department of Mechanical, Aerospace, and Nuclear Engineering.

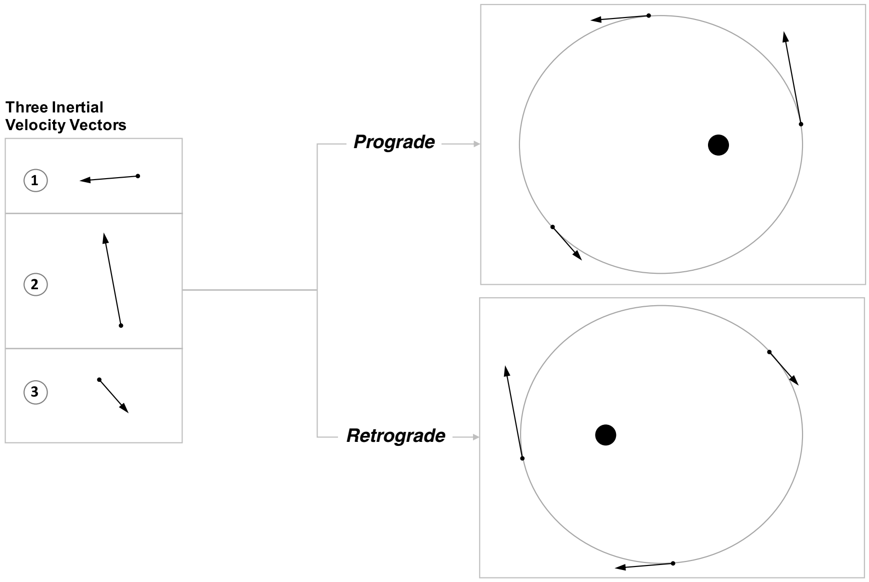

Fig. 1 There are exactly two orbits that could explain a sequence of three velocity vector observations: one prograde and one retrograde. Specification of the direction of motion makes the solution unique.

$$\mathcal{E} = \frac{\|\boldsymbol{v}\|^2}{2} - \frac{\mu}{\|\boldsymbol{r}\|} \tag{3}$$

and the eccentricity vector $\boldsymbol{e}$ is given by

$$\mu\boldsymbol{e} = \boldsymbol{v} \times \boldsymbol{h} - \frac{\mu}{\|\boldsymbol{r}\|}\boldsymbol{r} \tag{4}$$

The relations in Eqs. (2–4) may be applied to arrive at an analytic solution for IOD using only three velocity vectors. All three of these quantities ($\boldsymbol{h}$, $\mathcal{E}$, and $\boldsymbol{e}$) are conserved and must have the same values at all three measurement times. Therefore, the solution consists of three main steps: 1) compute the orbital plane; 2) decompose each unknown position vector into components parallel and perpendicular to the known velocity vector; and 3) use conservation of $\boldsymbol{h}$, $\boldsymbol{e}$, and $\mathcal{E}$ to compute remaining unknowns and find the position vector at each time. Each step is now discussed in detail, followed by a brief algorithm summary.

A. Compute Orbital Plane

The first step is to compute the orbital plane. Begin this task by recognizing that an object obeying two-body motion remains in an inertially fixed plane and all of the position vectors $\{\boldsymbol{r}_1, \boldsymbol{r}_2, \boldsymbol{r}_3\}$ and velocity vectors $\{\boldsymbol{v}_1, \boldsymbol{v}_2, \boldsymbol{v}_3\}$ must lie in this plane. Consequently, the unit normal to the orbit plane is given by

$$\boldsymbol{k} = \pm\frac{\boldsymbol{v}_1 \times \boldsymbol{v}_2}{\|\boldsymbol{v}_1 \times \boldsymbol{v}_2\|} = \pm\frac{\boldsymbol{v}_1 \times \boldsymbol{v}_3}{\|\boldsymbol{v}_1 \times \boldsymbol{v}_3\|} = \pm\frac{\boldsymbol{v}_2 \times \boldsymbol{v}_3}{\|\boldsymbol{v}_2 \times \boldsymbol{v}_3\|} \tag{5}$$

In the presence of measurement noise, however, simply computing the direction of $\boldsymbol{k}$ as the cross-product of two of the velocity vectors is not optimal in the least-squares sense. Therefore, the authors instead prefer to find the best-fit plane to all three velocity vectors that passes exactly through the origin and that minimizes the residuals orthogonal to the plane. This is equivalent to the total least-squares (TLS) fitting of a plane to a set of 3D points. The TLS problem has been widely studied, and the optimal solution may be found through a singular value decomposition [10,11].

To arrive at the TLS solution, observe that $\boldsymbol{k}$ is the unit vector ($\|\boldsymbol{k}\| = 1$) describing the one-dimensional null space of the 3×3 matrix $\boldsymbol{N}$,

$$\boldsymbol{N} = \begin{bmatrix} \boldsymbol{v}_1^T \\ \boldsymbol{v}_2^T \\ \boldsymbol{v}_3^T \end{bmatrix} \tag{6}$$

such that

$$\boldsymbol{N}\boldsymbol{k} = \boldsymbol{0}_{3\times 1} \quad \text{(noise free)} \tag{7}$$

$$\boldsymbol{N}\boldsymbol{k} = \boldsymbol{\epsilon} \quad \text{(noisy)} \tag{8}$$

where $\boldsymbol{\epsilon}$ is a vector of the residuals orthogonal to the plane. The TLS solution for $\boldsymbol{k}$ is found by taking the singular value decomposition $\boldsymbol{N} = \boldsymbol{U}\boldsymbol{D}\boldsymbol{V}^T$ and retaining the column of $\boldsymbol{V}$ corresponding to the smallest singular value in $\boldsymbol{D}$.

The singular value decomposition (SVD)-based solution method also makes clear a few requirements on the set of velocity vectors $\{\boldsymbol{v}_1, \boldsymbol{v}_2, \boldsymbol{v}_3\}$. Specifically, the 3×3 matrix $\boldsymbol{N}$ should have a one-dimensional null space, meaning that the velocity vectors should span a two-dimensional subspace (the orbital plane). Therefore, a solution will only be possible when velocity vectors are sufficiently well separated in direction to make the orbital plane well defined. Two velocity vectors may be collinear (e.g., one at periapsis and one at apoapsis) so long as they are not nearly repeated (e.g., both at nearly the same point on the orbit or both along the asymptote of a hyperbolic orbit in which the velocity vector is not changing) and the third velocity vector is pointed in a sufficiently different direction to fully define the plane.

The direction of $\boldsymbol{k}$ at this point is still arbitrary. To make things simpler later on, choose the direction of $\boldsymbol{k}$ to be the same as the angular momentum, leading to $\boldsymbol{h} = h\boldsymbol{k}$ (where $h = \|\boldsymbol{h}\|$). Choosing the correct direction requires additional information beyond the list of three velocity vectors. Depending on the orbit, this information may be available in a few different ways.

First, assuming the orbit is not nearly polar, it is often known if the spacecraft is in a prograde or retrograde orbit. In such a situation, it is possible to choose the direction of $\boldsymbol{k}$ according to

$$\begin{cases} \boldsymbol{\omega}^T\boldsymbol{k} > 0 & \text{prograde} \\ \boldsymbol{\omega}^T\boldsymbol{k} < 0 & \text{retrograde} \end{cases} \tag{9}$$

where $\boldsymbol{\omega}$ is the angular momentum vector describing the central body's rotation. This requires no knowledge of the ordering or timing of the velocity vectors.

In other situations, the ordering of the three velocity vectors is known. In this scenario, the ordering may be used to determine the direction of motion if bounds can be placed on the change in eccentric anomaly E between a pair of velocity measurements. Specifically, select the sign of $\boldsymbol{k}$ such that

$$\begin{cases} (\boldsymbol{v}_i \times \boldsymbol{v}_j)^T \boldsymbol{k} > 0 & 0 \ \text{deg} < E_j - E_i < 180 \ \text{deg} \\ (\boldsymbol{v}_i \times \boldsymbol{v}_j)^T \boldsymbol{k} < 0 & \text{otherwise} \end{cases} \tag{10}$$

where $\boldsymbol{v}_i$ and $\boldsymbol{v}_j$ are not collinear.

Finally, a third scenario is when the timing of each velocity vector measurement is known. Here, a direction of motion may be assumed, and the IOD problem may be solved. With the orbit known, Kepler's problem may be solved to find the expected time of flight between the various measurement locations and compared with the actual times of flight. If the expected and measured times of flight are in approximate agreement, then the solution is correct. If not, the alternate direction of motion should be selected, and the times of flights should be reevaluated.

B. Decomposition of Position Vector

With the orbital plane known, the position vectors (which must lie in this plane) may be decomposed into a component parallel to the velocity vector and a component perpendicular to the velocity vector. Therefore, define the direction parallel to the velocity vector by the unit vector $\boldsymbol{u}_i$,

$$\boldsymbol{u}_i = \frac{\boldsymbol{v}_i}{\|\boldsymbol{v}_i\|} \tag{11}$$

and the direction perpendicular to the velocity vector (and in the orbital plane) by the unit vector $\boldsymbol{w}_i$,

$$\boldsymbol{w}_i = \frac{\boldsymbol{u}_i \times \boldsymbol{k}}{\|\boldsymbol{u}_i \times \boldsymbol{k}\|} \tag{12}$$

where $\boldsymbol{k}$ is obtained from the SVD-based solution to Eq. (8). The components, therefore, are

$$\boldsymbol{r}_{u_i} = (\boldsymbol{u}_i^T \boldsymbol{r}_i)\boldsymbol{u}_i = (\boldsymbol{u}_i \boldsymbol{u}_i^T)\boldsymbol{r}_i \qquad \text{(parallel component)} \tag{13}$$

$$\boldsymbol{r}_{w_i} = (\boldsymbol{w}_i^T \boldsymbol{r}_i)\boldsymbol{w}_i = (\boldsymbol{w}_i \boldsymbol{w}_i^T)\boldsymbol{r}_i \qquad \text{(perpendicular component)} \tag{14}$$

such that the position vector may be written as

$$\boldsymbol{r}_i = \boldsymbol{r}_{u_i} + \boldsymbol{r}_{w_i} \tag{15}$$

A graphical depiction of this geometry is shown in Fig. 2.

C. Solve for Unknown Position Vectors

Solving for the full position vectors requires the application of the conservation of momentum, the eccentricity vector, and energy.

Therefore, proceed by considering the conservation of specific angular momentum at each measurement time,

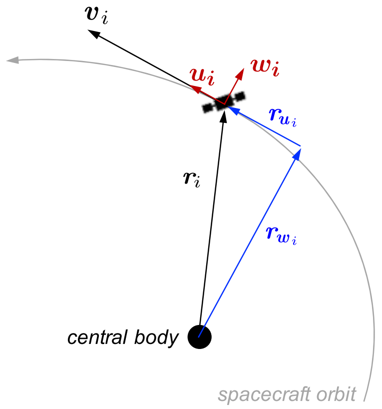

Fig. 2 Orbit geometry and decomposition of position vector by velocity direction (as viewed in the orbital plane).

$$\boldsymbol{h} = \boldsymbol{r}_i \times \boldsymbol{v}_i \tag{16}$$

which, letting $h = \|\boldsymbol{h}\|$, is the same as

$$\boldsymbol{h} = h\boldsymbol{k} = \boldsymbol{r}_{w_i} \times \boldsymbol{v}_i \tag{17}$$

Since $\boldsymbol{r}_{w_i}$ is perpendicular to $\boldsymbol{v}_i$ by construction,

$$h\boldsymbol{k} = \|\boldsymbol{r}_{w_i}\|\|\boldsymbol{v}_i\|\boldsymbol{k} \tag{18}$$

leading to the scalar relation that

$$\frac{\|\boldsymbol{r}_{w_i}\|}{h} = \frac{1}{\|\boldsymbol{v}_i\|} \tag{19}$$

Therefore, defining the intermediate variable z_i as

$$z_i = \frac{\boldsymbol{r}_{w_i}}{h} = \frac{\|\boldsymbol{r}_{w_i}\|}{h}\boldsymbol{w}_i \tag{20}$$

one arrives at

$$z_i = \frac{1}{\|\boldsymbol{v}_i\|}\boldsymbol{w}_i \tag{21}$$

where $\boldsymbol{v}_i$ is given and $\boldsymbol{w}_i$ is known from Eq. (12).

Continue by recalling the expression for the eccentricity vector,

$$\mu\boldsymbol{e} = \boldsymbol{v}_i \times \boldsymbol{h} - \frac{\mu}{\|\boldsymbol{r}_i\|}\boldsymbol{r}_i \tag{22}$$

which may be rewritten as

$$\mu\boldsymbol{e} = (\|\boldsymbol{v}_i\|\boldsymbol{u}_i) \times (h\boldsymbol{k}) - \frac{\mu}{\|\boldsymbol{r}_i\|}\boldsymbol{r}_i \tag{23}$$

and, observing from Eq. (12) that $\boldsymbol{w}_i = \boldsymbol{u}_i \times \boldsymbol{k}$ since each $\boldsymbol{u}_i$ is perpendicular to $\boldsymbol{k}$ in the absence of noise, rewritten again as

$$\mu\boldsymbol{e} = h\|\boldsymbol{v}_i\|\boldsymbol{w}_i - \frac{\mu}{\|\boldsymbol{r}_i\|}\boldsymbol{r}_i \tag{24}$$

Additionally, expand $\boldsymbol{r}_i$ in the last term into its components,

$$\mu\boldsymbol{e} = h\|\boldsymbol{v}_i\|\boldsymbol{w}_i - \frac{\mu}{\|\boldsymbol{r}_i\|}(\boldsymbol{r}_{\boldsymbol{u}_i} + \boldsymbol{r}_{\boldsymbol{w}_i}) \tag{25}$$

Divide both sides by the constant $h = \|\boldsymbol{h}\|$, and recall Eq. (20),

$$\mu\frac{\boldsymbol{e}}{h} = \|\boldsymbol{v}_i\|\boldsymbol{w}_i - \frac{\mu}{\|\boldsymbol{r}_i\|}\left(\frac{\boldsymbol{r}_{\boldsymbol{u}_i}}{h} + z_i\right) \tag{26}$$

Although it may not be immediately evident, the only unknowns on the right-hand side of Eq. (26) are two scalars. Define these unknown scalars as α_i and β_i,

$$\alpha_i = \frac{\mu}{\|\boldsymbol{r}_i\|} \tag{27}$$

$$\beta_i = \gamma_i\frac{\mu}{\|\boldsymbol{r}_i\|}\frac{\|\boldsymbol{r}_{\boldsymbol{u}_i}\|}{h} \tag{28}$$

where $\gamma_i = \pm 1$ such that $\boldsymbol{r}_{u_i} = \gamma_i\|\boldsymbol{r}_{u_i}\|\boldsymbol{u}_i$. The variable γ_i is necessary since it is possible for $\boldsymbol{r}_{u_i}$ to be in the opposite direction of $\boldsymbol{u}_i$. Note that $\alpha_i > 0$ by construction. Now, it is possible to rewrite Eq. (26) as

$$\mu\frac{\boldsymbol{e}}{h} = \|\boldsymbol{v}_i\|\boldsymbol{w}_i - \alpha_i z_i - \beta_i\boldsymbol{u}_i \tag{29}$$

where, once again, it is noted that α_i and β_i are the only unknowns on the right-hand side. Since the quantity $\mu\boldsymbol{e}/h$ is conserved, it follows that

$$\|\boldsymbol{v}_i\|\boldsymbol{w}_i - \alpha_i \boldsymbol{z}_i - \beta_i \boldsymbol{u}_i = \|\boldsymbol{v}_j\|\boldsymbol{w}_j - \alpha_j \boldsymbol{z}_j - \beta_j \boldsymbol{u}_j \tag{30}$$

or, equivalently, after isolating terms containing unknowns on the left-hand side,

$$\alpha_i \boldsymbol{z}_i + \beta_i \boldsymbol{u}_i - \alpha_j \boldsymbol{z}_j - \beta_j \boldsymbol{u}_j = \|\boldsymbol{v}_i\|\boldsymbol{w}_i - \|\boldsymbol{v}_j\|\boldsymbol{w}_j \tag{31}$$

for $\{i, j\}$ pairs $\{1,2\}$, $\{1,3\}$, and $\{2,3\}$. This produces nine equations, only four of which are algebraically independent. Since there are six unknowns (α_i and β_i for $i = \{1,2,3\}$), two more algebraically independent equations are required to find a solution.

The remaining two equations may be found from the *vis viva* equation,

$$\mathcal{E} = \frac{\|\boldsymbol{v}_i\|^2}{2} - \frac{\mu}{\|\boldsymbol{r}_i\|} = \frac{\|\boldsymbol{v}_i\|^2}{2} - \alpha_i \tag{32}$$

Again, for $\{i, j\}$ pairs $\{1,2\}$, $\{1,3\}$, and $\{2,3\}$, one has

$$\frac{\|\boldsymbol{v}_i\|^2}{2} - \alpha_i = \frac{\|\boldsymbol{v}_j\|^2}{2} - \alpha_j \tag{33}$$

which is rearranged to

$$\alpha_i - \alpha_j = \frac{\|\boldsymbol{v}_i\|^2}{2} - \frac{\|\boldsymbol{v}_j\|^2}{2} \tag{34}$$

producing three equations, two of which are independent. With the relations from Eqs. (31) and (34), it is now possible to form a linear system to solve for α_i and β_i. Form the 6×1 vector $\boldsymbol{g}$,

$$\boldsymbol{g} = [\alpha_1 \quad \beta_1 \quad \alpha_2 \quad \beta_2 \quad \alpha_3 \quad \beta_3]^T \tag{35}$$

such that the linear system becomes

$$\begin{bmatrix} \boldsymbol{z}_1 & \boldsymbol{u}_1 & -\boldsymbol{z}_2 & -\boldsymbol{u}_2 & \boldsymbol{0}_{3\times1} & \boldsymbol{0}_{3\times1} \\ \boldsymbol{z}_1 & \boldsymbol{u}_1 & \boldsymbol{0}_{3\times1} & \boldsymbol{0}_{3\times1} & -\boldsymbol{z}_3 & -\boldsymbol{u}_3 \\ \boldsymbol{0}_{3\times1} & \boldsymbol{0}_{3\times1} & \boldsymbol{z}_2 & \boldsymbol{u}_2 & -\boldsymbol{z}_3 & -\boldsymbol{u}_3 \\ 1 & 0 & -1 & 0 & 0 & 0 \\ 1 & 0 & 0 & 0 & -1 & 0 \\ 0 & 0 & 1 & 0 & -1 & 0 \end{bmatrix} \boldsymbol{g} = \begin{bmatrix} \|\boldsymbol{v}_1\|\boldsymbol{w}_1 - \|\boldsymbol{v}_2\|\boldsymbol{w}_2 \\ \|\boldsymbol{v}_1\|\boldsymbol{w}_1 - \|\boldsymbol{v}_3\|\boldsymbol{w}_3 \\ \|\boldsymbol{v}_2\|\boldsymbol{w}_2 - \|\boldsymbol{v}_3\|\boldsymbol{w}_3 \\ \|\boldsymbol{v}_1\|^2/2 - \|\boldsymbol{v}_2\|^2/2 \\ \|\boldsymbol{v}_1\|^2/2 - \|\boldsymbol{v}_3\|^2/2 \\ \|\boldsymbol{v}_2\|^2/2 - \|\boldsymbol{v}_3\|^2/2 \end{bmatrix} \tag{36}$$

where $\boldsymbol{z}_i$ is from Eq. (21), $\boldsymbol{u}_i$ is from Eq. (11), $\boldsymbol{w}_i$ is from Eq. (12), and $\boldsymbol{v}_i$ is known. Obtain a solution for $\boldsymbol{g}$ by solving the overdetermined system in Eq. (36) in the least-squares sense.

Therefore, with α_i and β_i known from the elements of $\boldsymbol{g}$, one can immediately solve for $\|\boldsymbol{r}_i\|$ by rearranging Eq. (27),

$$\|\boldsymbol{r}_i\| = \frac{\mu}{\alpha_i} \tag{37}$$

Returning to Eq. (15), observe that the position magnitude may be written in terms of its orthogonal components,

$$\|\boldsymbol{r}_i\|^2 = \|\boldsymbol{r}_{\boldsymbol{u}_i}\|^2 + \|\boldsymbol{r}_{\boldsymbol{w}_i}\|^2 \tag{38}$$

Now, divide by h^2,

$$\frac{\|\boldsymbol{r}_i\|^2}{h^2} = \left(\frac{\beta_i}{\alpha_i}\right)^2 + \|\boldsymbol{z}_i\|^2 \tag{39}$$

such that one can rearrange to find the magnitude of the specific angular momentum h,

$$h^2 = \frac{\|\boldsymbol{r}_i\|^2}{\|\boldsymbol{z}_i\|^2 + (\beta_i/\alpha_i)^2} \tag{40}$$

Further, recalling from Eq. (21) that $\|\boldsymbol{z}_i\| = 1/\|\boldsymbol{v}_i\|$,

$$h^2 = \frac{\|\boldsymbol{r}_i\|^2\|\boldsymbol{v}_i\|^2}{1 + \|\boldsymbol{v}_i\|^2(\beta_i/\alpha_i)^2} \tag{41}$$

$$h = \|\boldsymbol{r}_i\|\|\boldsymbol{v}_i\|\left[1 + \left(\frac{\beta_i\|\boldsymbol{v}_i\|}{\alpha_i}\right)^2\right]^{-1/2} \tag{42}$$

Note that if the measurements of $\boldsymbol{v}_i$ are noisy then a different value for h will be computed for each measurement time. While any number of conventions could be chosen, the authors choose to simply take the average value of h among the three measurement times.

With h known, one simply has to rewrite Eqs. (20) and (28) for the components of $\boldsymbol{r}_i$ to obtain the solution

$$\boldsymbol{r}_{\boldsymbol{w}_i} = h\boldsymbol{z}_i \tag{43}$$

$$\boldsymbol{r}_{\boldsymbol{u}_i} = \frac{\beta_i h\|\boldsymbol{r}_i\|}{\mu}\boldsymbol{u}_i \tag{44}$$

where

$$\boldsymbol{r}_i = \boldsymbol{r}_{\boldsymbol{u}_i} + \boldsymbol{r}_{\boldsymbol{w}_i} \tag{45}$$

D. Algorithm Summary

A brief summary outlining the solution procedure for performing IOD with only three velocity vectors is provided in Table 1.

While the present Note focuses on the IOD solution using only three velocity vectors, the extension to simultaneously processing a larger ($n \geq 4$) number of measurements is straightforward. One only needs to include the additional velocity measurements when finding $\boldsymbol{k}$ with Eq. (8) (the SVD approach naturally handles the resulting rectangular system) and in constructing the linear system in Eq. (36) (being careful to include all unique $\{i, j\}$ pairs and noting that $\boldsymbol{g}$ becomes a $2n \times 1$ vector). The rest of the solution procedure is identical.

IV. Discussion and Numerical Results

The IOD from the three velocity vector solution method summarized in Sec. III.D was validated and assessed through a number of numerical studies. These studies are presented in the following subsections.

A. Example Orbit Determination with Perfect Measurements

The first step in evaluating any new IOD method is to demonstrate that it can exactly recover the true orbit when provided perfect measurements. This was found to be the case for the solution to IOD from three velocity vectors summarized in Sec. III.D, in which the true solution was recovered to within machine precision for all examples tested by the authors. The new IOD method was found to work equally well for circular, elliptical, and hyperbolic orbits. A small sampling of the cases examined by the authors is now provided as examples.

Consider a simulated spacecraft in Earth orbit undergoing perfect two-body motion. Let the spacecraft be in a prograde orbit with perigee radius of 7178.1 km, inclination of 30 deg, argument of periapsis of 70 deg, and right ascension of the ascending node of 40 deg. Let the eccentricity vary to create examples of a circular orbit ($e = 0$), an elliptical orbit ($e = 0.4$), a parabolic orbit ($e = 1.0$), and a hyperbolic orbit ($e = 1.2$).

Table 1 Algorithm summary for IOD from three velocity vectors

Step 1:	Obtain three velocity vector measurements $\{\boldsymbol{v}_1, \boldsymbol{v}_2, \boldsymbol{v}_3\}$, and specify the direction of motion.
Step 2:	Compute the orbital plane normal vector $\boldsymbol{k}$ by the SVD-based solution to Eq. (8) with the direction chosen according to the discussion in Sec. III.A.
Step 3:	Form $\boldsymbol{u}_i$ [Eq. (11)] and $\boldsymbol{w}_i$ [Eq. (12)] for $i = \{1, 2, 3\}$.
Step 4:	Compute $\{z_1, z_2, z_3\}$ using Eq. (21).
Step 5:	Compute α_i and β_i for $i = \{1, 2, 3\}$ (six components of the $\boldsymbol{g}$ vector) as the least-squares solution to Eq. (36).
Step 6:	Find $\|\boldsymbol{r}_i\|$ for $i = \{1, 2, 3\}$ using Eq. (37).
Step 7:	Compute h using Eq. (42).
Step 8:	Compute $\boldsymbol{r}_i$ for $i = \{1, 2, 3\}$ using Eqs. (43–45).
Step 9:	Having found inertial position vectors at all three times, the IOD problem is complete.

Table 2 IOD-produced position estimates are correct to within machine precision when all three velocity measurements are perfect

			Normalized error		
Orbit type	Measurement time	True anomaly	$\delta r_x/\|\boldsymbol{r}_i\|$	$\delta r_y/\|\boldsymbol{r}_i\|$	$\delta r_z/\|\boldsymbol{r}_i\|$
Circular	t_1	20 deg	8.2357×10^{-16}	1.5204×10^{-15}	5.0681×10^{-16}
($e = 0.0$)	t_2	60 deg	-7.6022×10^{-16}	-3.9595×10^{-16}	3.8011×10^{-16}
	t_3	100 deg	0.0000×10^{-16}	-1.0770×10^{-15}	-3.1676×10^{-16}
Elliptical	t_1	47 deg	1.1491×10^{-16}	8.0435×10^{-16}	2.8727×10^{-16}
($e = 0.4$)	t_2	107 deg	-3.2029×10^{-16}	0.0000×10^{-16}	1.4513×10^{-16}
	t_3	138 deg	0.0000×10^{-16}	-3.8035×10^{-16}	-2.5357×10^{-16}
Parabolic	t_1	37 deg	6.8295×10^{-16}	-1.7074×10^{-15}	-5.6912×10^{-16}
($e = 1.0$)	t_2	80 deg	2.0738×10^{-15}	1.2928×10^{-15}	-1.4775×10^{-16}
	t_3	100 deg	2.5238×10^{-15}	2.8392×10^{-15}	5.1264×10^{-16}
Hyperbolic	t_1	110 deg	-4.4653×10^{-15}	-2.7062×10^{-15}	1.1269×10^{-15}
($e = 1.2$)	t_2	129 deg	-4.9234×10^{-15}	-9.6229×10^{-15}	-2.1260×10^{-15}
	t_3	134 deg	-6.9346×10^{-15}	-1.6820×10^{-14}	-4.6476×10^{-15}

Given three velocity measurements placed around the example orbits, the IOD method is used to find the unknown position vectors at the corresponding times. In all cases, the unknown position vectors at all three times are recovered to within machine precision as shown in Table 2.

B. Performance Assessment

Measurements are never perfect, and the results from Sec. IV.A must be extended to consider how IOD performance degrades as the velocity measurements are corrupted by noise. Unfortunately, the solution procedure outlined in Sec. III.D does not lend itself to a compact analytic expression for the position estimate covariance. In the absence of such an analytic solution, the authors numerically assessed the performance through a variety of Monte Carlo analyses. First, results from a single scenario were assessed. Second, many different scenarios were considered (varying eccentricity, spacing of velocity observations, and measurement noise), and performance contours were created.

For the first case, consider the circular orbit example from Sec. IV.A, with velocity measurements spaced as described in Table 2 and with a measurement standard deviation of $\sigma_v = 1.0\ \mathrm{m/s}$. Scatter plots of the IOD-produced position residuals corresponding to the center velocity measurement (at t_2) are shown in Fig. 3 for a 1000-run Monte Carlo.

For the second case, consider two orbits: one circular ($e = 0$) and one elliptical ($e = 0.5$). For each of these two orbits, allow the velocity measurement separation (in terms of mean anomaly ΔM) to vary from 0 to 120 deg and velocity measurement noise σ_v to vary from 1 cm/s to 10 m/s. As a point of reference, observe that velocity errors on the order of $\sigma_v = 3\ \mathrm{m/s}$ were achieved in [6]. The three velocity measurements are assumed to be equidistant in mean anomaly, such that $\Delta M = M_2 - M_1 = M_3 - M_2$. For each scenario (combination of eccentricity, ΔM, and σ_v), a 10,000-run Monte Carlo was performed. In each case, the rms of the errors was computed for the following quantities using the position estimate at t_2: 3D position, orbit semimajor axis, and flight-path angle. Contours for these rms errors are shown in Figs. 4–6.

As expected, an increase in noise on the velocity measurements results in deterioration of orbit determination performance. While the optimal spacing between velocity measurements is dependent on the eccentricity of the orbit, larger spacing between the measurements generally produces a better IOD solution.

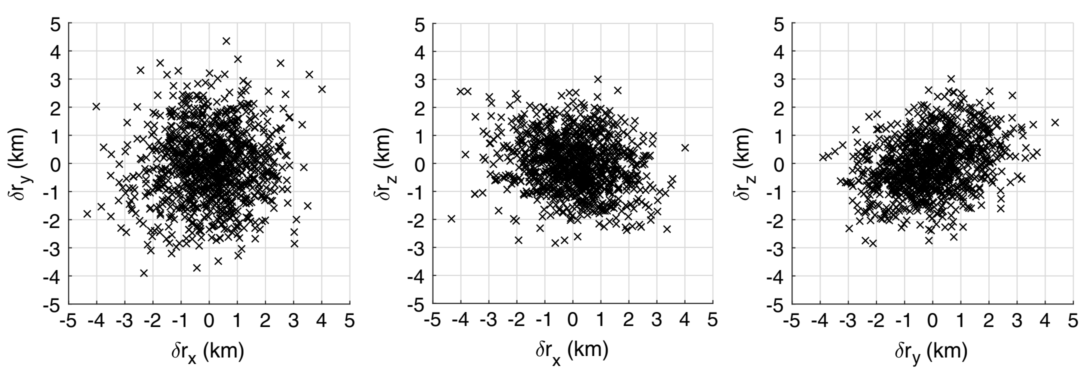

Fig. 3 Position errors corresponding to center velocity measurement (at t_2) for velocity-only IOD in circular orbit.

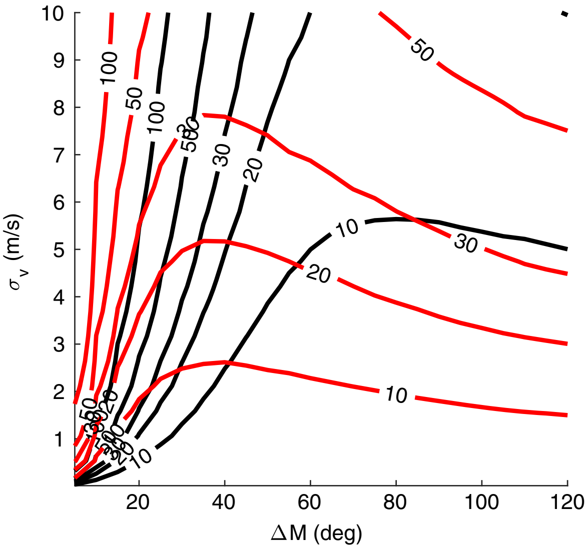

Fig. 4 Contours of rms of position residuals in kilometers for a circular orbit (black lines) and an elliptical orbit (red lines).

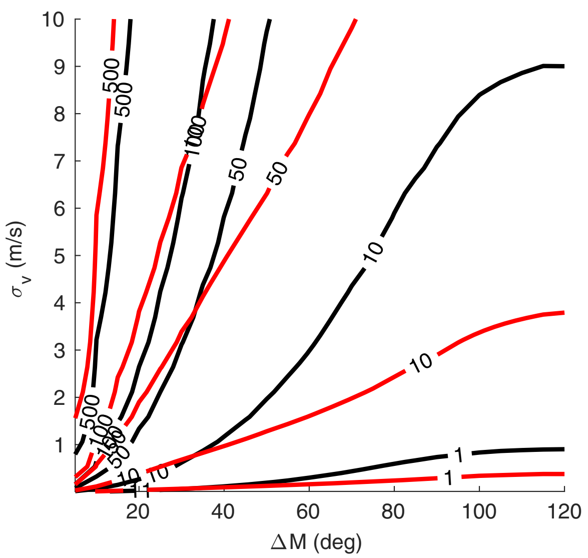

Fig. 5 Contours of rms of semimajor axis residuals in kilometers for a circular orbit (black lines) and an elliptical orbit (red lines).

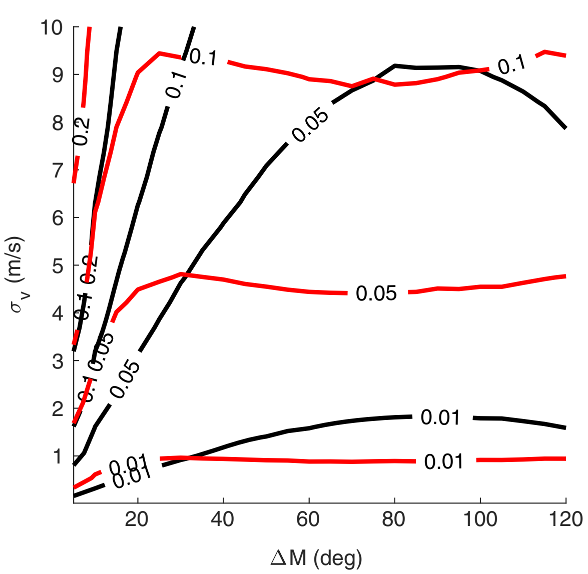

Fig. 6 Contours of rms of flight-path angle residuals in degrees for a circular orbit (black lines) and an elliptical orbit (red lines).

V. Conclusions

This Note considers the problem of initial orbit determination given only three velocity vectors. The astute reader can quickly observe this to be similar to the classic initial orbit determination (IOD) problem given three position vectors (Gibbs problem), where the knowns and unknowns have been switched. Although the present work was motivated by velocity measurements from X-ray navigation, the velocity-only IOD approach developed here is valid for any future system capable of obtaining inertial velocity measurements.

An analytic solution to the problem of IOD from only three velocity vectors was derived, and the final solution procedure was found to be a straightforward sequence of simple computations. If desired, the solution may be easily adapted to handle four or more velocity vector measurements, processing them all together in the least-squares sense. The analytic IOD solution works for all types of two-body orbits (circular, elliptical, parabolic, and hyperbolic). Numerical studies demonstrated that a computer implementation of this algorithm produces the correct solution to within machine precision for objects undergoing two-body motion and with perfect (noise-free) velocity measurements. The same algorithm is capable of processing noisy velocity measurements, with kilometer-level positioning possible in some useful scenarios.

Acknowledgments

The authors thank Zach Putnam and Kevin Lohan from the University of Illinois at Urbana–Champaign for insightful discussions on X-ray navigation. The authors also thank Shane Robinson from NASA Johnson Space Center for being a reliable sounding board for new ideas.

References

[1] Battin, R., *An Introduction to the Mathematics and Methods of Astrodynamics*, rev. ed., AIAA, Reston, VA, 1999, pp. 114–117, 131–133, 295–342.

[2] Vallado, D., *Fundamentals of Astrodynamics and Applications*, 4th ed., Microcosm, Hawthorne, CA, 2013, pp. 450–457, 464–495.

[3] Escobal, P., *Methods of Orbit Determination*, Krieger, Malabar, FL, 1965, pp. 239–290.

[4] Gooding, R., "A New Procedure for the Solution of the Classical Problem of Minimal Orbit Determination from Three Lines of Sight," *Celestial Mechanics & Dynamical Astronomy*, Vol. 66, 1997, pp. 387–423.
doi:10.1007/BF00049379

[5] Sheikh, S., Pines, D., Ray, P., Wood, K., Lovellette, M., and Wolff, M., "Spacecraft Navigation Using X-Ray Pulsars," *Journal of Guidance, Control, and Dynamics*, Vol. 29, No. 1, 2006, pp. 49–63.
doi:10.2514/1.13331

[6] Winternitz, L., Mitchell, J., Hassouneh, M., Valdez, J., Price, S., Semper, S., Yu, W., Ray, P., Wood, K., and Arzoumanian, Z., et al., "SEXTANT X-Ray Pulsar Navigation Demonstration: Flight System and Test Results," *IEEE Aerospace Conference*, IEEE Publ., Piscataway, NJ, March 2016.
doi:10.1109/AERO.2016.7500838

[7] Mitchell, J., Winternitz, L., Hassouneh, M., Price, S., Semper, S., Yu, W., Ray, P., Wolff, M., Kerr, M., and Wood, K., et al., "SEXTANT X-Ray Pulsar Navigation Demonstration: Initial On-Orbit Results," *AAS Guidance and Control Conference*, American Astronautical Soc. Paper 18-155, Springfield, VA, 2018.

[8] Winternitz, L., Mitchell, J., Hassouneh, M., Price, S., Semper, S., Yu, W., Ray, P., Wolff, M., Kerr, M., and Wood, K., et al., "SEXTANT X-Ray Pulsar Navigation Demonstration: Additional On-Orbit Results," *SpaceOps Conference*, AIAA Paper 2018-2538, 2018,
doi:10.2514/6.2018-2538

[9] Sheikh, S., "The Use of Variable Celestial X-Ray Sources for Spacecraft Navigation," Ph.D. Thesis, Univ. of Maryland, College Park, MD, 2005, pp. 220–238.

[10] Markovsky, I., and Van Huffel, S., "Overview of Total Least-Squares Methods," *Signal Processing*, Vol. 87, No. 10, 2007, pp. 2283–2302.
doi:10.1016/j.sigpro.2007.04.004

[11] Christian, J., "Optical Attitude Determination from Horizon Orientation Using Image Segmentation," *Journal of Guidance, Control, and Dynamics*, Vol. 36, No. 1, 2013, pp. 113–123.
doi:10.2514/1.57222